

## Evaluation of the enrichment and amplification effect of pentachlorobenzene with lower bioconcentration in the food chain before and after modification

Ruihao SUN<sup>1</sup>, Meijin DU<sup>1</sup>, Yu LI\*<sup>1</sup>

MOE Key Laboratory of Resources and Environmental Systems Optimization,  
North China Electric Power University, Beijing, P.R. China

Received: 27.06.2019

Accepted/Published Online: 24.09.2019

Final Version: 09.12.2019

**Abstract:** In this paper, in order to construct a 3D quantitative structure–activity relationship (QSAR) model with the chlorobenzene (CB) molecular structure parameter as an independent variable and the octanol-water partition coefficient ( $K_{OW}$ ) as a dependent variable, 9 kinds of CB molecules were used as training sets and 3 kinds of CB molecules were used as test sets. We adopted the QSAR module in the Sybyl-X2.0 software from the Tripos Corporation (USA). The molecular modification of the pentachlorobenzene molecule with low bioconcentration was carried out by combining a three-dimensional contour map and fractional factorial design. The results showed that the toxicity, migration, and enrichment of 17 new pentachlorobenzene molecules with low bioconcentration decreased and their degradability increased; it was also found that the concentration and amplification effect of the pentachlorobenzene molecules in the food chain decreased after modification when compared with unmodified pentachlorobenzene, which was determined by docking premodified and modified pentachlorobenzene molecules with enzymes in living organisms in a food chain (*Chlamydomonas reinhardtii* → *Daphnia pulex* → *Danio rerio* → pelican). Furthermore, the enrichment capacity of the modified pentachlorobenzene in some edible animals (such as pigs, cows, sheep, chickens, ducks, rabbits, and fish) also decreased.

**Key words:** Pentachlorobenzene, molecular modification, bioconcentration, molecular docking

### 1. Introduction

Chlorobenzenes (CBs) are a class of aromatic chlorides in which a hydrogen atom is replaced by a chlorine atom on a benzene ring; depending on the number and position of the chlorine atoms in the benzene ring, there are 12 homologues. Chlorobenzenes are a kind of synthetic organic compound that exist in the environment; these molecules are very stable with regard to physical and chemical properties and are not easily degraded [1]. The pollution characteristics of chlorobenzene organics include a low degradation rate, easy enrichment by biological accumulation, and persistence as a highly toxic pollutant [2]. With the universal detection of CBs in the environment and the continuous occurrence of related environmental pollution events, research on CBs has attracted extensive attention.

CBs have been used in dyes, medicines, pesticides, organic synthesis, and other industries [3], and their presence in soil, water, sediment, activated sludge, and other environmental media has been detected [4]. The Stockholm Convention listed hexachlorobenzene as a persistent organic pollutant (POPs) in May 2001 and listed pentachlorobenzene in May 2009 [5]; hexachlorobenzene, pentachlorobenzene, 1,2,4,5-tetrachlorobenzene, and

\*Correspondence: liyuxx8@hotmail.com

1,2,4-trichlorobenzene have also been added to the US Environmental Protection Agency's list of 31 pollutants for priority control [6]. Pentachlorobenzene, as an organic source of chlorobenzene, has been used as an insecticide, flame retardant, and insulating fluid, and it is also used in the synthesis of pentachloronitrobenzene [7]; furthermore, pentachlorophenol, an organic pollutant derived from pentachlorobenzene, has attracted attention worldwide because of its strong neurotoxicity, carcinogenicity, and organ-sensitivity [8].

The octanol-water partition coefficient ( $K_{OW}$ ) can reflect the ability of organics to distribute in the octanol phase and aqueous phase, and it is also one of the important parameters used to study the environmental behavior of organic matter and the distribution behavior of organics in biologics and water [9].  $K_{OW}$  can be simulated, and this value is closely related to the toxicity [10,11], bioconcentration, and solubility of the compounds [12,13]. The research objects of the quantitative structure-activity relationship (QSAR) include the biological activity [14], various physical and chemical properties [15], environmental behaviors [16], and toxicity and bioavailability of compounds [17,18], and its research fields include chemistry, biology, pharmacy, and environmental sciences [19]. The study of 3D-QSAR is based on the three-dimensional structural characteristics of ligands and receptors, and the relationship between three-dimensional structure and biological activity can be quantitatively analyzed according to the internal energy of molecules and the energy changes of intermolecular interactions [20]. 3D-QSAR has been used in the fields of biochemistry [21], biomedicine [22], ecotoxicology [23], oncology [24], antimicrobial agents, and metabolism based on three-dimensional analysis [25,26]. Comparative molecular field analysis (CoMFA) and hypothetical active site lattice approaches are the common research methods used for 3D-QSAR [27].

In this study, a 3D-QSAR model (CoMFA and comparative molecular similarity index analysis (CoMSIA)) based on CB bioconcentration ( $K_{OW}$ ) data was established and combined with a fractional factorial design of 17 new CB molecules with low biodegradability, low mobility, low toxicity, and high degradability that were selected by using 2D-QSAR and molecular docking technology to analyze CB molecules regarding the enrichment mechanisms of organisms.

## 2. Materials and methods

### 2.1. Data sources

The molecular  $K_{OW}$  experimental data for the 12 kinds of CBs were introduced from the EPIWEB database, and the logarithm  $\log K_{OW}$  of  $K_{OW}$  was taken as the indicator of the CBs' enrichment ability. According to a ratio of 3:1, 9 data points were randomly selected as the training set, and the remaining 3 data points were selected as the test set [28,29]. A 3D-QSAR model for CB bioconcentration was then constructed. The selected enzymes in this study were all obtained from the Protein Data Bank (<http://www ww p d b . o r g />).

### 2.2. Main research methods

QSAR models with good fit and good robustness were established by different modeling methods and variable combinations, and molecular modification sites were determined by a fractional factorial and three-dimensional equipotential map. Thus, the key factors affecting molecular bioconcentration were identified to help with the CB molecular design to produce molecules with low bioconcentrations. The bioconcentration mechanism of the molecules in organisms were studied by the methods of 2D-QSAR and molecular docking.

### 3. Results

#### 3.1. Construction, prediction, validation, and analysis of the CB bioconcentration ( $K_{OW}$ ) QSAR model

##### 3.1.1. Construction and evaluation of the QSAR model

Two models of CoMFA and CoMSIA were selected, and the influence rates are shown in Table 1.

**Table 1.** Molecular field's contribution to CBs'  $K_{OW}$  of the CoMFA and CoMSIA models.

Model	S	E	H	D	A
CoMFA	43.2%	56.8%	-	-	-
CoMSIA	0.7%	86.1%	13.2%	0	0

As shown in Table 1, in the CoMFA model, the influence rates of the three-dimensional field (S) and static electric field (E) on the CB molecules are 43.2% and 56.8%, respectively, showing that the space effect and the electrical effect both influence the  $K_{OW}$  of the CB homologues and that the electrical effect is more significant than the space effect. In the CoMSIA model, the influence rates of the three-dimensional field (S), electrostatic field (E), hydrophobic field (H), hydrogen bond donor field (D), and hydrogen bond receptor field (A) on the chlorobenzene molecules are 0.70%, 86.10%, 13.20%, 0.00%, and 0.00%, respectively, indicating that the spatial effect, the electric effect, and the hydrophobic effect are influential on the  $K_{OW}$  of CB molecules. The electric effect is the main influencing factor.

The evaluation parameters of the CoMFA and CoMSIA models are shown in Table 2.

**Table 2.** Evaluation parameters of the CoMFA and CoMSIA models.

Model	n	$q^2$	$r^2$	SEE	F	$r^2_{pred}$	SEP	Q2
CoMFA	7	0.980	1.000	0.028	1156.369	0.975	0.188	0.188
CoMSIA	5	0.989	1.000	0.026	1896.781	0.977	0.180	0.326

As shown in Table 2, the optimal principal component n of the CoMFA model is 7, and the optimal principal component n of the CoMSIA model is 5. The cross-validation coefficient  $q^2$  of the CoMFA model is 0.980, and that of the CoMSIA model is 0.989; both coefficients are greater than 0.500, indicating that the predictive ability of the model is relatively high. The non-cross-validation coefficient  $R^2$  is 1.000 for both the CoMFA and CoMSIA models, showing that the predictive results of the two models have high fitting ability and good stability [30].

##### 3.1.2. Verification and prediction of the QSAR model

The established CoMFA and CoMSIA models were used to predict the activity of the tested set of molecules to verify the accuracy of the models. According to Gu et al., both models include a linear relationship between the predicted values and experimental values [31]; the predicted values and experimental values of the linear fitting correlation coefficients are high at 0.998 and 0.992, respectively, showing that the goodness of fit of the predicted values and experimental values are higher and that the two models have high internal prediction ability. From the statistical parameters of the model fitting degree of interaction, the external prediction set interaction test

coefficient  $r_{pred}^2$  had values of 0.975 and 0.977, respectively, showing that the models have high stability and a good prediction ability. Thus, these models can be used to predict the  $K_{OW}$  of the CB molecules.

The  $K_{OW}$  values of the 12 kinds of CB molecules were predicted by the CoMFA model and CoMSIA model, respectively, and the predicted results are shown in Table 3.

**Table 3.** Predicted  $K_{OW}$  values of CBs based on CoMFA and CoMSIA models.

Compounds	Obs.	CoMFA		CoMSIA	
		Pred.	RE (%)	Pred.	RE (%)
Monochlorobenzene	2.840	2.844	0.141	2.844	0.141
1,2-Dichlorobenzene	3.430	3.444	0.408	3.452	0.641
1,3-Dichlorobenzene	3.526	3.513	-0.369	3.526	0.000
1,4-Dichlorobenzene	3.440	3.249	-5.552	3.206	-6.802
1,2,3-Trichlorobenzene	4.050	4.041	-0.222	4.033	-0.420
1,2,4-Trichlorobenzene	4.020	3.976	-1.095	3.986	-0.846
1,3,5-Trichlorobenzene	4.190	4.19	0.000	4.910	17.184
1,2,3,4-Tetrachlorobenzene	4.600	4.619	0.413	4.573	-0.587
1,2,4,5-tetrachlorobenzene	4.640	4.626	-0.302	4.617	-0.496
1,2,3,5-Tetrachlorobenzene	4.560	4.551	-0.197	4.549	-0.241
Pentachlorobenzene	5.170	5.184	0.271	5.195	0.484
Hexachlorobenzene	5.730	5.735	0.087	5.733	0.052

### 3.1.3. Analysis of factors influencing the molecular bioconcentration of CBs based on a three-dimensional equipotential diagram

The molecular skeleton structure of the CBs is shown in Figure 1.

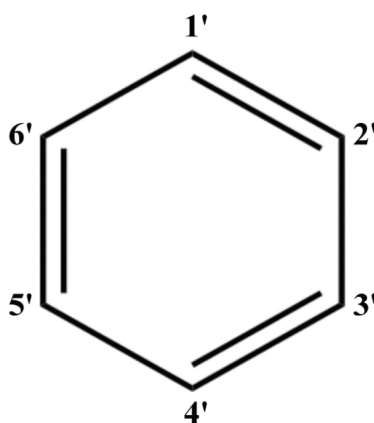


**Figure 1.** Molecular skeleton structure of CBs.

The three-dimensional equipotential diagrams of the CoMFA and CoMSIA models of pentachlorobenzene molecules were analyzed using the pentachlorobenzene molecule as the target molecule. As shown in Figure 2, in the steric field, the green region indicates that the introduction of a substituent larger than Cl in this region

will improve the bioconcentration of pentachlorobenzene. In the electrostatic field, the red region indicates that the introduction of a substituent with stronger electronegativity than Cl in this region will improve the bioconcentration of pentachlorobenzene.

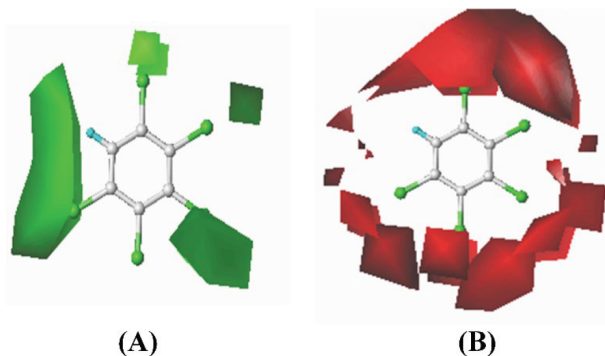


**Figure 2.** Contour maps of CoMFA model: steric fields (A), electrostatic fields (B).

As shown in Figure 2A, in the equipotential diagram of the steric field the green region is distributed around the substituents at  $R_1$ ,  $R_3$ ,  $R_5$ , and  $R_6$ , indicating that the introduction of substituents larger than Cl into these positions will increase the bioconcentration of pentachlorobenzene. For example, the bioconcentration of 1,2,4,5-tetrachlorobenzene is lower than that of pentachlorobenzene because the volume of substituent H at  $R_3$  of 1,2,4,5-tetrachlorobenzene is less than that of the Cl substituent at  $R_3$  of pentachlorobenzene. As shown in Figure 2B, in the equipotential diagram of the electrostatic field, the red region is distributed around the substituents at  $R_1$ ,  $R_2$ ,  $R_3$ ,  $R_4$ , and  $R_5$ , indicating that the introduction of more electronegative groups than Cl at this position will increase the bioconcentration of pentachlorobenzene. For example, the bioconcentration of 1,2,3,5-tetrachlorobenzene is less than that of pentachlorobenzene because the electronegativity of the H substituent at  $R_4$  of 1,2,3,5-tetrachlorobenzene is less than that of the Cl substituent of pentachlorobenzene  $R_4$ .

As shown in Figure 3, in the steric field, the green region indicates that the introduction of a substituent larger than Cl in this region will improve the bioconcentration of pentachlorobenzene. In the electrostatic field, the red region indicates that the introduction of a substituent with stronger electronegativity than Cl in this region will improve the bioconcentration of pentachlorobenzene. In the hydrophobic field, the yellow region indicates that the introduction of a hydrophobic substituent stronger than Cl in this region will improve the bioconcentration of pentachlorobenzene.

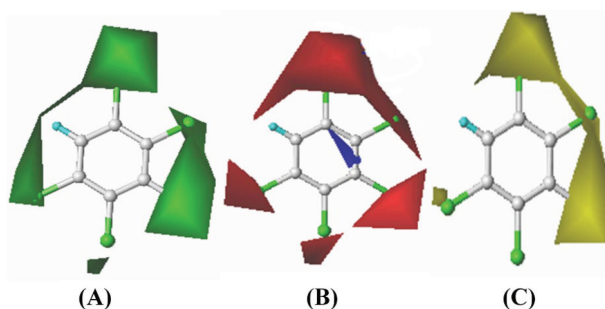


**Figure 3.** Contour maps of CoMSIA model: steric fields (A), electrostatic fields (B), hydrophobic fields (C).

In Figure 3A, in the equipotential diagram of the steric field, the green region is distributed around the substituents at R<sub>1</sub>, R<sub>2</sub>, R<sub>3</sub>, and R<sub>5</sub>, indicating that the introduction of a substituent with a smaller volume than Cl in this position will reduce the bioconcentration of pentachlorobenzene. For example, the bioconcentrations of 1,2,3,4-tetrachlorobenzene, 1,2,4,5-tetrachlorobenzene, and 1,2,3,5-tetrachlorobenzene are lower than the bioconcentration of pentachlorobenzene because the volume of substituent H at positions R<sub>5</sub>, R<sub>3</sub>, and R<sub>4</sub> is smaller than that of substituent Cl.

In Figure 3B, in the equipotential diagram of the electrostatic field, the red region is distributed around the substituents at R<sub>1</sub>, R<sub>2</sub>, R<sub>3</sub>, R<sub>4</sub>, and R<sub>5</sub>, indicating that the introduction of a substituent with a stronger electronegativity than Cl at this position can improve the bioconcentration of pentachlorobenzene.

In Figure 3C, in the equipotential diagram of the hydrophobic field, the yellow region is distributed around the substituents at R<sub>1</sub>, R<sub>2</sub>, and R<sub>3</sub>, indicating that the introduction of a substituent with a larger hydrophobicity than Cl at this position will increase the bioconcentration of pentachlorobenzene.

### **3.2. Determination of low-bioconcentration pentachlorobenzene substitution sites, functional evaluation, and evaluation of POPs characteristics of the modified molecules**

#### **3.2.1. Determination of low-bioconcentration pentachlorobenzene substitution sites based on 3D-QSAR and fractional factorial design**

A fractional factorial design was used to research the main effects, two-factor interactions, and three-factor interaction effects between different substitution sites to obtain a standard effect diagram to determine substitution sites. Du et al. investigated the effect of different substitution sites of pentachlorobenzene in regard to its enrichment with the help of Minitab software and adopted the fractional factorial design [32]. According to the analysis of the equipotential diagram, the structural modification information reflected by the equipotential diagram and fractional factorial was basically the same, but the blocky regions of the equipotential diagram were scattered and the molecular field was widely distributed, which makes it difficult to accurately locate the molecular field's influence region. Therefore, the more accurate fractional factorization combined with the equipotential diagram was used to modify the molecule.

#### **3.2.2. Evaluation of flame retardancy and insulation properties of the modified molecules**

The positive frequency, bond dissociation enthalpy, and optical energy gap of the modified molecules were calculated using Gaussian 09, and the results are shown in Table 4.

In Table 4, the positive frequency, bond dissociation enthalpy, and optical energy gap were calculated for the modified molecules, and we found that the positive frequency of 3-tert-butyl-6-ethyl-pentachlorobenzene is  $-11.87 < 0$ , the positive frequency of 3-amino-6-isopropyl-pentachlorobenzene is  $-347.38 < 0$ , and the positive frequencies of the other molecules are all greater than 0, indicating that most of these molecules can be stable. To test how the flame retardancy and insulation properties of the modified molecules compared with those of the target molecule, the bond dissociation enthalpy and optical energy gap of pentachlorobenzene and the modified molecules, which represent the flame retardancy and insulation properties, were calculated using Gaussian 09. The lower the enthalpy is, the stronger the flame retardancy; the higher the optical energy gap is, the stronger the insulation properties. Geometric optimization of all compounds was performed at the b3pw91/6-31 g\* level using density functional theory. The changing range of the bond dissociation enthalpy of the modified molecule compared with the target molecule is  $-14.946\%$  to  $6.762\%$ , indicating that the flame retardancy of the modified molecules did not change obviously. The changing range of the optical energy gap compared with the target

**Table 4.** The positive frequency, bond dissociation enthalpy, and optical energy gap of the modified molecules.

Compounds	Positive-freq.	Bond disso.	RE (%)	Optical energy gap	RE (%)
Pentachlorobenzene	68.56	86.499	-	0.209	-
2-Methyl-pentachlorobenzene	77.53	88.035	1.775	0.213	1.865
3-Methyl-pentachlorobenzene	68.49	87.657	1.339	0.214	2.343
4-Methyl-pentachlorobenzene	67.79	87.877	1.592	0.212	1.387
3-Tert-butyl-6-methyl-pentachlorobenzene	8.33	73.572	-14.946	0.214	2.343
3-Tert-butyl-6-ethyl-pentachlorobenzene	-11.87	-	-	-	-
3-Ethyl-6-methyl-pentachlorobenzene	69.37	88.725	2.573	0.217	3.778
3-Methyl-6-methyl-pentachlorobenzene	34.92	89.073	2.975	0.216	3.300
3-Methyl-6-ethyl-pentachlorobenzene	45.85	88.402	2.199	0.217	3.778
3-Tert-butyl-4-ethyl-pentachlorobenzene	32.53	88.331	2.117	0.208	-0.526
3-Tert-butyl-4-methyl-pentachlorobenzene	23.39	88.549	2.369	0.212	1.387
3-Methyl-4-methyl-pentachlorobenzene	46.35	88.078	1.825	0.216	3.300
3-Methyl-4-tert-butyl-pentachlorobenzene	40.94	86.571	0.083	0.203	-2.917
3-Methyl-4-ethyl-pentachlorobenzene	69.11	88.227	1.997	0.216	3.300
3-Amino-6-hydroxy-pentachlorobenzene	88.86	90.634	4.780	0.179	-14.395
3-Amino-6-isopropyl-pentachlorobenzene	-347.38	-	-	-	-
3-Amino-6-isopropyl-pentachlorobenzene	54.46	84.234	-2.619	0.195	-6.743
2-Methyl-4-ethyl-5-tert-butyl-pentachlorobenzene	33.11	73.940	-14.520	0.217	3.778
2-Hydroxy-4-amino-5-isopropyl-pentachlorobenzene	55.21	84.297	-2.547	0.204	-2.439
2-Isopropyl-4-amino-5-hydroxy-pentachlorobenzene	26.42	92.349	6.762	0.199	-4.830

molecule is -14.395% to 3.778%, indicating that there is also no significant change in the insulation properties of the modified molecules. Compared with the target molecule, the modified molecules had almost no change in functional characteristics.

### 3.2.3. Evaluation of the toxicity, mobility, and degradability of the modified molecules

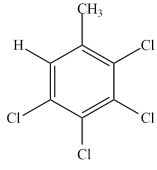
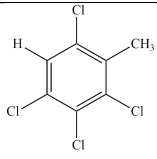
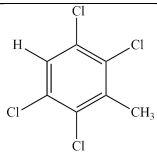
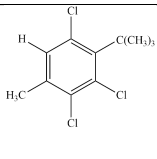
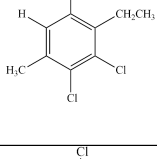
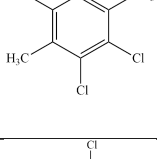
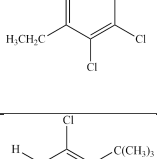
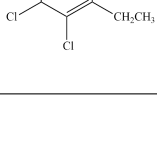
To test whether the properties of the other POPs changed after modification, the toxicity ( $-\log EC_{50}$ ) and migration ( $\log K_{OA}$  and  $\log t_{1/2}$ ) of the CB molecular  $K_{OW}$ s were predicted by the 3D-QSAR models developed in this paper. The evaluation parameters of the models are shown in Table 5.

**Table 5.** Models statistical parameters of  $-\log EC_{50}$ ,  $\log K_{OA}$ , and  $\log t_{1/2}$ .

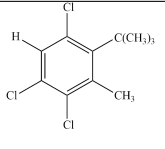
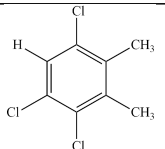
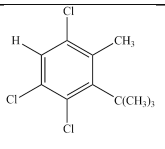
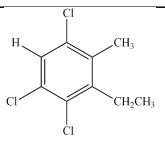
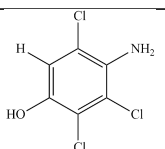
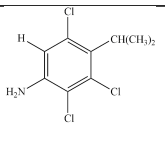
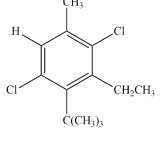
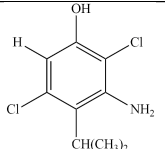
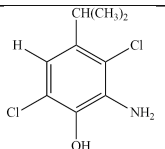
Models	n	q <sup>2</sup>	r <sup>2</sup>	SEE	F	r <sub>pred</sub> <sup>2</sup>	SEP
$-\log EC_{50}$	5	0.846	0.995	0.119	77.505	0.842	0.371
$\log K_{OA}$	2	0.951	0.992	0.130	360.353	0.871	0.561
$\log t_{1/2}$	7	0.728	0.999	0.035	142.422	0.772	0.306

The prediction results of the modified molecules'  $\log K_{OA}$ ,  $\log K_{OW}$ ,  $-\log EC_{50}$ , and  $\log t_{1/2}$  are shown in Table 6.

**Table 6.** Predicted values of molecular modified  $\log K_{OW}$ ,  $-\log EC_{50}$ ,  $\log K_{OA}$ , and  $\log t_{1/2}$ .

No.	Compounds	$\log K_{OW}$		$\log K_{OA}$		$-\log EC_{50}$		$\log t_{1/2}$	
		CoMSIA	RE (%)	CoMSIA	RE (%)	CoMSIA	RE (%)	CoMFA	RE (%)
1		4.45	13.93	5.55	14.48	5.04	12.20	2.54	30.36
2		4.27	17.41	5.74	11.56	5.58	2.79	2.63	27.89
3		4.25	17.79	5.27	18.80	4.83	15.85	2.09	42.70
4		4.38	15.28	5.54	14.64	5.37	6.45	2.73	25.15
5		3.78	26.89	4.66	28.20	5.09	11.32	3.39	7.06
6		3.76	27.27	4.63	28.66	5.04	12.20	3.64	0.20
7		3.93	23.98	4.87	24.96	4.85	15.51	3.04	16.65
8		4.92	4.84	5.63	13.25	5.26	8.36	2.62	28.17



9		4.96	4.06	5.55	14.48	5.24	8.71	2.43	33.38
10		3.53	31.72	4.71	27.43	4.258	25.82	2.80	23.23
11		4.73	8.51	5.65	12.94	5.49	4.36	3.03	16.93
12		3.67	29.01	4.96	23.57	4.79	16.55	3.18	12.81
13		4.30	16.83	5.43	16.33	5.48	4.53	2.46	32.55
14		3.74	27.66	4.80	26.04	4.39	23.52	3.64	0.20
15		4.21	18.57	4.54	30.05	4.59	20.03	2.21	39.41
16		3.86	25.34	4.73	27.12	4.47	22.13	2.25	38.31
17		4.35	15.86	4.65	28.35	4.71	17.94	3.08	15.56

There are many factors that affect the bioconcentration of CB molecules. In this paper, 17 novel molecules were obtained by modifying pentachlorobenzene. According to the model predictions, the  $\log K_{OW}$  value of the modified molecules was significantly reduced, with a maximum reduction of 31.70%. Their mobility and toxicity were reduced and their degradability was increased, indicating that the modified molecules conform to the concepts of environmentally friendly molecules.

### 3.3. Bioconcentration mechanism analysis before and after pentachlorobenzene modification based on the 2D-QSAR model

Obtaining the molecular structure parameters is one of the key steps in the study of 2D-QSAR, and it is very important to select the appropriate structural parameters for the establishment of the model. According to studies on the relationship between the structural parameters of pentachlorobenzene and the bioconcentration of the modified compounds, such as that conducted by Yang et al., it has been found that selection of the appropriate quantitative parameters can be performed by continuously establishing regression equations [33]. Parameters of the pentachlorobenzene molecules before and after modification were calculated by Gaussian 09 software. Quantized parameters, such as dipole moment ( $\mu$ , Debye), optical energy gap ( $V$ ), most negative density charge number ( $q^-$ , e), the most positive density charge number ( $q^+$ , e), molecular energy ( $TE$ , eV), highest occupied molecular orbital ( $E_{HOMO}$ ), and lowest occupied molecular orbital ( $E_{LUMO}$ ), were obtained as independent variables, and taking the  $\log K_{OW}$  data as the dependent variable, the multiple linear regression equation was established using SPSS. Finally, the dipole moment ( $\mu$ , Debye), optical energy gap ( $V$ ), most negative density charge number ( $q^-$ , e), most positive density charge number ( $q^+$ , e), and molecular energy ( $TE$ , eV) were selected, and the 2D-QSAR model of bioconcentration before and after molecular modification was established. According to the data standardization formula, the equation relating  $\log K_{OW}$  to the quantum chemical parameters before and after molecular modification can be derived as follows:

Molecular equation of CBs before modification:

$$\log K_{OW} = 28.42 - 0.165\mu + 82.36V + 99.583q^- - 10.854q^+ \quad (1)$$

Molecular equation of CBs after modification:

$$\log K_{OW} = 83.693 + 0.026\mu - 220.661V - 129.682q^+ + 19.369q^- + 8.548 \times 10^{-4}TE \quad (2)$$

For the 2D-QSAR model representing molecular bioconcentration,  $R^2$  was 0.821 and 0.893 ( $>0.8$ ), and Sig was 0.042 and 0.023 ( $<0.05$ ), and all of these values passed the significance test [34]. From Eq. (1), the most negative density charge number is the main factor affecting the bioconcentration of molecules before modification, while from Eq. (2), the optical energy gap is the main factor affecting the bioconcentration of molecules after modification. By analyzing the CB molecular equation established before and after molecular modification, the  $\log K_{OW}$  parameter equation for the modified CB molecules is related to the dipole moment ( $\mu$ , Debye), optical energy gap ( $V$ ), most negative density charge number ( $q^-$ , e), most positive density charge number ( $q^+$ , e), and molecular energy ( $TE$ , eV), while the bioconcentration equation before molecular modification has nothing to do with the quantization parameter of molecular energy ( $TE$ , eV). These results indicate that the decrease in the bioconcentration of the modified molecule might be caused by the change in molecular energy. The parameter coefficients of the dipole moment and the most negative density charge number are positive, while the optical energy gap, most positive density charge number, and molecular energy

have negative values for the molecules after modification. These results show that the molecular dipole moment and the most negative density charge number have positive effects on the bioconcentration of the modified molecules, the optical energy gap, and the most positive density charge number, while the molecular energy has negative effects on the bioconcentration of the modified molecules.

### 3.4. Risk assessment of the enrichment of pentachlorobenzene in organisms before and after modification based on molecular docking technology

#### 3.4.1. Risk assessment of the enrichment of pentachlorobenzene in the food chain before and after modification

Molecular docking is a technique that simulates the binding of pollutant molecules to proteins in organisms, and the scoring function is used to judge the strength of their ability to combine. The enrichment of pollutant molecules in organisms was analyzed, and the differences of enrichment ability before and after molecular modification were compared in the organisms. The chlorobenzene organic pollutants were enriched and amplified through the food chain [35]. In this article, four species were selected: *Chlamydomonas reinhardtii*, *Daphnia pulex*, *Danio rerio*, and pelican, which can form a food chain in nature (*C. reinhardtii* → *D. pulex* → *D. rerio* → pelican). It is possible to reduce the concentration of pollutants in the human body by reducing the enrichment at each trophic level of the food chain [36].

As shown in Table 7, the pentachlorobenzene scoring function values of enzymes in *C. reinhardtii*, *D. pulex*, *D. rerio*, and pelican are 1.2939, 1.041, 0.899, and 0.307, respectively. It can be seen from the data that the binding ability of pentachlorobenzene to the enzymes in *C. reinhardtii* is higher because the selected enzymes are degrading enzymes; as the molecule is better able to bind the enzymes, the score of the function value is higher and thus the pollutants are less likely to accumulate in organisms. The algae are at the very bottom of the food chain. If we can reduce the ability of pollutants to accumulate in algae, then the concentration of pollutants in organisms at high nutrient levels can be effectively reduced, as can the toxicity of pollutants to organisms. The mean score functions of enzymes in *C. reinhardtii*, *D. pulex*, *D. rerio*, and pelican with the modified molecules are 2.563, 2.220, 1.841, and 1.383, respectively. It can be seen from the data that when the modified molecules are compared with the target molecule (pentachlorobenzene), their ability to bind to enzymes in organisms has been greatly improved, indicating that the enrichment capacity of the pollutants is reduced in organisms. For example, except for the score function value of 3-methyl-pentachlorobenzene (No. 2), docking with enzymes being reduced in *C. reinhardtii*, the degree of improvement is obvious. For example, the molecular improvement effect of 3-methyl-6-ethyl-pentachlorobenzene (No. 7) and 3-methyl-4-ethyl-pentachlorobenzene (No. 12) reached 160.298% and 168.413%, respectively.

In Figure 4, for the modified molecules in the food chain, the enrichment ability is reduced at each trophic level, and in addition, the amplification process is lower than it was before the modification, indicating that the degree of damage to organisms after molecular modification is reduced.

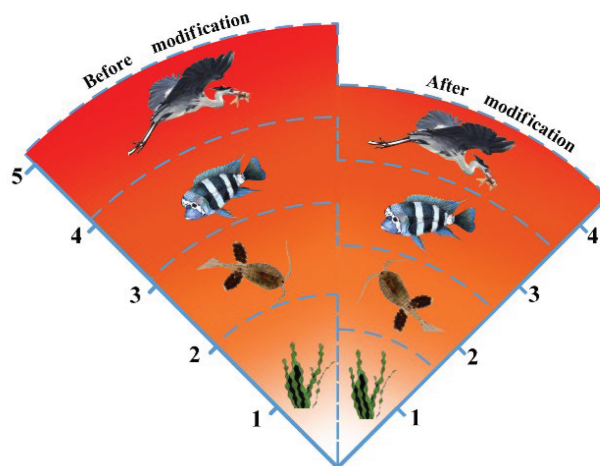
#### 3.4.2. Enrichment capacity analysis of pentachlorobenzene in some organisms before and after modification

*Sus scrofa*, *Bos taurus*, *Ovis aries*, *Danio rerio*, *Gallus gallus*, *Anas platyrhynchos*, and *Oryctolagus cuniculus* are directly edible animals, so reducing the enrichment of pollutants in these organisms can effectively reduce the enrichment capacity of pollutants in the human body. The following animal species are abundant and have a certain representative classification: *S. scrofa* (omnivorous animal); *B. taurus*, *O. aries*, and *O. cuniculus*

**Table 7.** The score function values of enzymes in the food chain before and after modification of pentachlorobenzene.

No.	<i>C. reinhardtii</i>		<i>D. pulex</i>		<i>D. rerio</i>		Pelican	
	Dock score	RE (%)	Dock score	RE (%)	Dock score	RE (%)	Dock score	RE (%)
PeCB	1.293	-	1.041	-	0.899	-	0.307	-
1	2.011	55.422	2.108	102.498	1.656	84.205	0.804	161.889
2	0.921	-28.819	1.905	82.997	1.872	108.231	0.799	160.261
3	1.820	40.660	2.724	161.671	1.249	38.932	0.686	123.453
4	3.102	139.740	1.665	59.942	1.571	74.750	1.018	231.596
5	2.564	98.161	1.605	54.179	2.500	178.087	1.204	292.182
6	2.587	99.938	2.220	113.256	2.001	122.581	1.515	393.485
7	3.368	160.298	2.869	175.600	1.645	82.981	1.451	372.638
8	2.950	127.993	3.123	200.000	1.477	64.294	1.639	433.876
9	3.211	148.164	4.572	339.193	1.680	86.874	1.358	342.345
10	2.706	109.135	1.019	-2.113	2.600	189.210	1.67	443.974
11	2.827	118.487	1.601	53.794	1.794	99.555	1.483	383.062
12	3.473	168.413	2.780	167.051	2.570	185.873	0.993	223.453
13	2.457	89.891	0.212	-79.635	2.417	168.854	1.366	344.951
14	2.242	73.275	2.207	112.008	1.373	52.725	1.288	319.544
15	2.349	81.544	2.275	118.540	1.303	44.939	1.967	540.717
16	2.767	113.850	2.954	183.766	1.580	75.751	2.994	875.244
17	2.081	60.832	1.914	83.862	2.017	124.360	1.278	316.287

PeCB: pentachlorobenzene.

**Figure 4.** Amplification of risk assessment in the food chain before and after pentachlorobenzene modification.

(herbivorous animals); *D. rerio* (aquatic animal); and *G. gallus* and *A. platyrhynchos* (poultry animals). As shown in Table 8 and Table 9, the enrichment capacity of a large number of molecules after modification was decreased compared with that before modification, and the enrichment capacity of the polysubstituted molecules was significantly lower than that of the monosubstituted molecules, thus supporting the design philosophy for environmentally friendly molecules. As shown in Figure 5, the enrichment capacities after molecular modification

in *S. scrofa*, *B. taurus*, *O. aries*, *D. rerio*, *G. gallus*, *A. platyrhynchos*, and *O. cuniculus* were all decreased by different degrees, and the average degree of decrease was more obvious in *A. platyrhynchos*, *O. aries*, and *S. scrofa*.

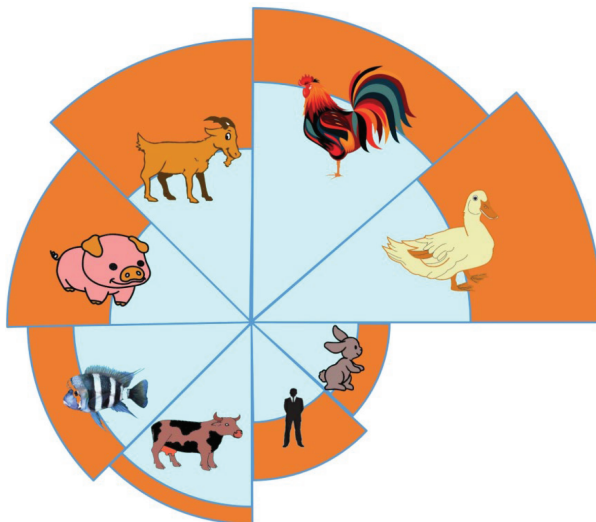


**Figure 5.** Schematic diagram of enrichment capacity of pentachlorobenzene in organisms before and after modification (blue area + orange area represents the enrichment capacity of pentachlorobenzene in organisms before modification, while blue area represents the enrichment capacity of pentachlorobenzene after modification).

### 3.5. Bioconcentration mechanism of pentachlorobenzene before and after modification based on amino acid residues analysis

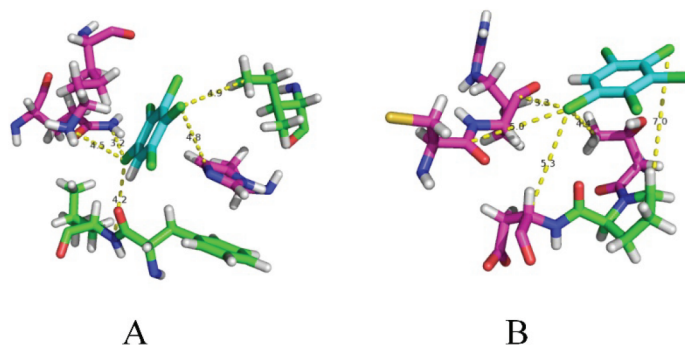
Molecular docking technology is used to study the binding of molecules to enzymes, and the binding ability of the molecule to the enzymes was analyzed according to the results of the scoring function. The binding ability of molecules to enzymes depends on the sites selected at the time of binding, and the amino acid residues around different sites are different. In this study, hydrophilic and hydrophobic groups were taken as examples. The more hydrophobic groups there are around the molecule, the stronger the ability of the molecule to bind to the enzyme [37]. Taking pentachlorobenzene and 3-tert-butyl-6-methyl-pentachlorobenzene as examples (randomly selected), the enzyme binding capacities of *C. reinhardtii*, *D. pulex*, *D. rerio*, and pelican were analyzed to determine the molecular enrichment capacity in the physical body.

In Figure 6, the schematic diagram of pentachlorobenzene molecule binding to enzymes in *C. reinhardtii* (A) and *D. pulex* (B) is shown. In Figure 6A, the hydrophobic amino acid residues are mainly ILE27, LEU41, and PHE40, while the hydrophilic groups are HIS30, LYS58, and GLN53; in Figure 6B, the hydrophobic groups are PRO5, while the hydrophilic groups are CYS22, ARG23, THR4, and ASP6. Based on the number of hydrophobic groups around the binding site, we inferred that the binding ability of pentachlorobenzene to the enzyme in *C. reinhardtii* is stronger than that of pentachlorobenzene to the enzyme in *D. pulex*, which is consistent with the score of molecular docking technology (the score function of the pentachlorobenzene molecule binding to the enzyme in *C. reinhardtii* was 1.293 and the score function of the enzyme in *D. pulex* was 1.041). According to the distribution of hydrophobic amino acid residues around the molecule, the enzyme binding abilities of pentachlorobenzene in the organisms were as follows: *C. reinhardtii* > *D. pulex* > *D. rerio* > pelican.

**Table 8.** Enrichment capacity of pentachlorobenzene in common organisms before and after modification.

No.	<i>S. scrofa</i>		<i>O. aries</i>		<i>B. taurus</i>	
	Dock score	RE (%)	Dock score	RE (%)	Dock score	RE (%)
PeCB	0.775	-	0.760	-	0.968	-
1	1.054	36.000	1.214	59.660	1.645	69.850
2	0.655	-15.480	1.384	82.050	1.096	13.200
3	1.587	104.774	1.010	32.860	0.976	0.810
4	1.583	104.258	3.045	300.447	1.131	16.860
5	1.987	156.387	1.840	142.062	0.637	-34.080
6	2.439	214.710	1.676	120.439	0.791	-18.280
7	2.419	212.129	2.479	225.990	1.830	88.980
8	3.041	292.387	1.905	150.612	1.206	24.590
9	1.998	157.806	1.567	106.103	0.954	-1.520
10	1.823	135.226	2.056	170.459	2.001	106.621
11	2.235	188.387	2.538	233.816	1.848	90.890
12	3.142	305.419	1.331	75.010	0.950	-1.840
13	2.263	192.000	1.707	124.490	2.229	130.221
14	3.145	305.806	3.201	321.031	2.069	113.716
15	2.156	178.194	2.676	251.993	2.204	127.629
16	1.369	76.645	2.478	225.924	1.243	28.341
17	3.641	369.806	2.428	219.295	3.930	305.918

PeCB: pentachlorobenzene.

**Figure 6.** Schematic diagram of the distance between amino acid residues and pentachlorobenzene (before modification).

In Figure 7, a microscopic diagram of the binding of the 3-tert-butyl-6-methyl-pentachlorobenzene molecule to enzymes in *C. reinhardtii* (A) and *D. pulex* (B) is shown. In Figure 7A, the microstructures of 3-tert-butyl-6-methyl-pentachlorobenzene (No. 4) binding with enzymes in *C. reinhardtii* show that the hydrophobic amino acid residues around the enzyme binding site of *C. reinhardtii* were mainly ILE27, ALA60, and PRO62, and the hydrophilic amino acid residues around the site were mainly HIS19, ASN24, CYS18, GLN53, and LYS58. In Figure 7B, for the microstructures of 3-tert-butyl-6-methyl-pentachlorobenzene (No. 4) binding with enzymes in *D. pulex*, the hydrophobic amino acid residues around the enzyme binding site of the molecule in *D. pulex* were mainly PRO5, and the hydrophilic residues were mainly SER2, HIS3, and THR4. There

**Table 9.** Enrichment capacity of pentachlorobenzene in common organisms before and after modification.

No.	<i>G. gallus</i>		<i>O. cuniculus</i>		<i>A. platyrhynchos</i>		<i>H. sapiens</i>	
	Dock score	RE (%)	Dock score	RE (%)	Dock score	RE (%)	Dock score	RE (%)
PeCB	0.419	-	1.571	-	0.256	-	1.0711	-
1	0.585	239.689	1.728	9.994	0.405	258.258	2.455	129.194
2	0.677	261.720	1.400	-10.885	0.813	417.493	2.386	122.780
3	0.635	251.613	1.203	-23.425	0.553	315.736	2.254	110.391
4	0.114	127.264	1.858	18.269	1.358	630.379	4.020	275.278
5	0.428	202.151	2.049	30.426	0.785	406.521	3.181	196.947
6	1.181	382.127	2.146	36.601	1.246	586.685	3.125	191.728
7	1.047	350.203	2.076	32.145	2.712	1158.766	3.461	223.126
8	0.399	195.293	2.012	28.071	1.234	581.804	4.255	297.264
9	0.823	296.726	1.501	-4.456	0.313	222.218	4.068	279.796
10	0.921	320.072	2.170	38.129	1.610	728.817	3.516	228.251
11	0.383	191.613	1.451	-7.638	1.033	503.202	2.706	152.675
12	0.855	304.349	1.542	-1.846	0.375	246.505	4.169	289.198
13	0.358	185.472	3.587	128.326	0.358	239.711	2.995	179.572
14	0.190	145.329	2.845	81.095	1.236	582.702	3.831	257.642
15	1.587	479.188	3.095	97.008	1.129	540.765	4.366	307.656
16	1.294	409.295	2.630	67.409	1.179	560.328	4.016	274.914
17	1.355	423.728	3.509	123.361	0.964	476.533	5.001	366.941

PeCB: pentachlorobenzene.

are more hydrophobic amino acid residues and hydrophilic amino acid residues around the enzyme binding site in *C. reinhardtii*, but the ratio of hydrophobic amino acid residues to hydrophilic amino acid residues was higher than that for *D. pulex*. Therefore, it is concluded that the binding ability of the 3-tert-butyl-6-methyl-pentachlorobenzene molecule to enzymes in *C. reinhardtii* is higher than that of *D. pulex*, and this result is consistent with the scoring function value (the scoring function value of the enzyme in *C. reinhardtii* is 3.102 and the scoring function value of the enzyme in *D. pulex* is 1.665). Figure 8 shows a schematic diagram of the enzyme in *C. reinhardtii* docking with pentachlorobenzene and 3-tert-butyl-6-methyl-pentachlorobenzene (No. 4).

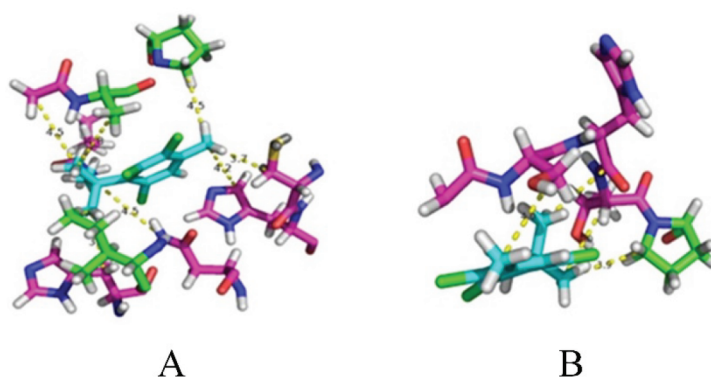


**Figure 7.** Schematic diagram of the molecular distance between amino acid residues and 3-tert-butyl-6-methyl-pentachlorobenzene (after modification).

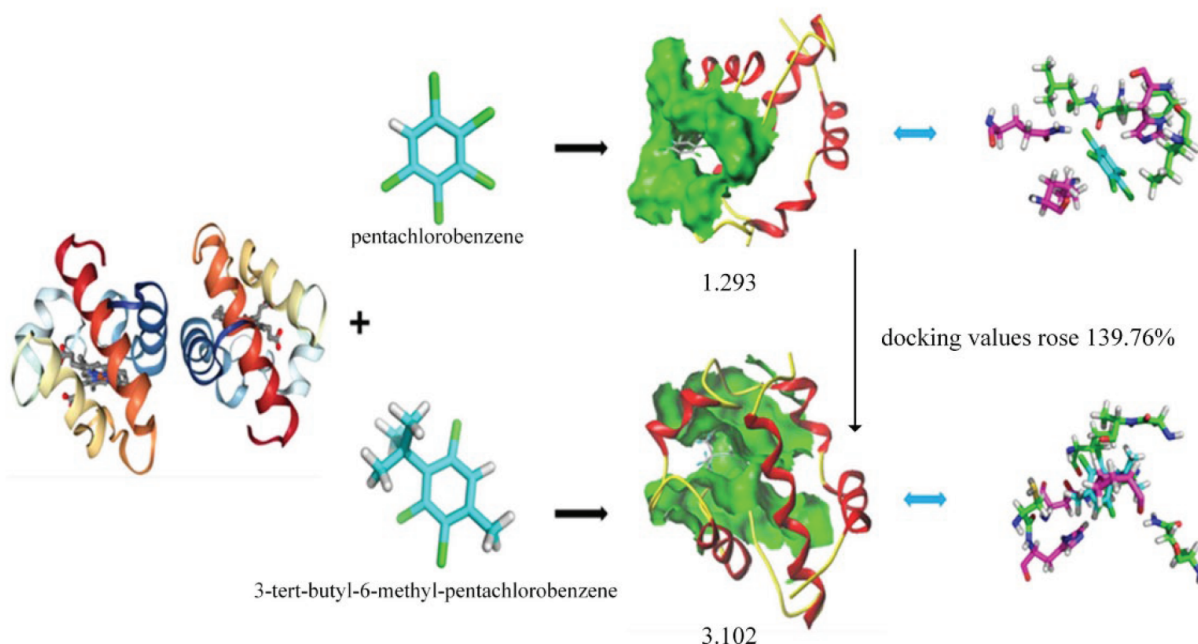


**Figure 8.** Schematic diagram of enzyme in *Chlamydomonas reinhardtii* docking with pentachlorobenzene and 3-tert-butyl-6-methyl-pentachlorobenzene.

To further explore the influence of the properties of amino acid residues on molecular docking, we performed a quantitative measurement of the distance between the amino acid residues and the molecules, and the calculation results are shown in Table 10 and Table 11.

**Table 10.** Distances between the hydrophilic residues and hydrophobic residues of pentachlorobenzene.

Compounds	Pentachlorobenzene			
	Hydrophilic residues	Distance	Hydrophobicresidues	Distance
<i>C. reinhardtii</i>	HIS30	4.8	ILE27	4.9
	LYS58	3.2	LEU41	4.2
	GLN53	4.5	PHE40	4.2
<i>D. pulex</i>	CYS22	5.0	PRO5	7.0
	ARG23	3.3	-	-
	THR4	4.4	-	-
	ASP6	5.3	-	-
<i>D. rerio</i>	CYS37	3.5	TYR39	4.0
	-	-	VAL81	4.7
	-	-	PRO82	5.6
Pelican	THR2	6.4	ALA1	4.0
	SER5	10.7	PRO3	3.9
	-	-	ALA4	8.8

From the perspective of amino acid residues, the binding abilities of molecules to enzymes in organisms were affected by the number of hydrophobic and hydrophilic groups around the binding site and the distance between these groups and the amino acid residues. The more hydrophobic amino acid residues located around



**Table 11.** Distances between the hydrophilic residues and hydrophobic residues of the modified molecules.

Compounds	3-tert-butyl-6-methyl-pentachlorobenzene (No. 4)			
	Hydrophilic residues	Distance	Hydrophobicresidues	Distance
<i>C. reinhardtii</i>	CYS18	3.7	PRO62	4.5
	HIS19	4.2	ILE27	3.7
	ASN24	4.5	ALA60	4.8
	GLN53	3.1	-	-
	LYS58	4.5	-	-
<i>D. pulex</i>	THR4	4	PRO5	3.9
	HIS3	4.7	-	-
	SER2	4.0	-	-
<i>D. rerio</i>	THR36	3.8	PRO38	5.3
	CYS37	3.6	TYR39	3.4
	THR80	4.4	VAL81	4.5
Pelican	THR2	4.3	ALA1	4.2
	-	-	PRO3	3.8
	-	-	ALA4	3.4

the docking site and the closer the distance between the docking molecules and the amino acid residues, the better the docking effect was.

#### 4. Conclusions

According to the 3D-QSAR model results, the established model has strong stability and a good prediction ability. Seventeen new CB molecules with low  $\log K_{OW}$  values were selected based on a three-dimensional contour map and fractional factorial design. The migration and toxicity of the novel CB molecules with low biological enrichment were reduced to a certain degree, their degradability was increased, and their functional characteristics remained basically unchanged.

Furthermore, the enrichment of premodified and modified pentachlorobenzene molecules was simulated by molecular docking technology, and it was found that the enrichment and amplification of the modified molecules in organisms through the food chain was significantly lower than that before molecular modification. At the same time, the study also found that the enrichment ability of modified molecules in some edible organisms also decreased to varying degrees, thus reducing the enrichment in the human body. From the perspective of 2D-QSAR and amino acid residues, the reasons for the differences in the enrichment ability of pentachlorobenzene and their derivatives in different organisms were explained.

#### Acknowledgment

This work was supported by the Key Projects in the National Science & Technology Pillar Program in the Eleventh Five-Year Plan Period [No. 2008BAC43B01].

## References

1. Brahusi F, Dörfler U, Shahinasi E, Schroll R, Munch J. The analyse of chlorobenzenes (CBs) in the soil environment. *Albanian Journal of Agricultural Sciences* 2013; 12 (2): 289-295.
2. Brahusi F, Kengara FO, Yang S, Xin J, Munch JC et al. Fate processes of chlorobenzenes in soil and potential remediation strategies: a review. *Pedosphere* 2017; 27 (3): 407-420. doi: 10.1016/S1002-0160(17)60338-2
3. Du QP, Ra XS, Huang CN. Chlorobenzenes in waterweeds from the Xijiang River (Guangdong section) of the Pearl River. *Journal of Environmental Sciences-China* 2007; 19 (10): 1171-1177. doi: 10.1016/S1001-0742(07)60191-0
4. Rapp P. Multiphasic kinetics of transformation of 1,2,4-trichlorobenzene at nano and micromolar concentrations by *Burkholderia* sp. strain PS14. *Applied and Environmental Microbiology* 2001; 67 (8): 3496-3500. doi: 10.1128/AEM.67.8.3496-3500.2001
5. Wei DB, Kameya T, Urano K. Environmental management of pesticidal POPs in China: past, present and future. *Environment International* 2007; 33 (7): 894-902. doi: 10.1016/j.envint.2007.04.006
6. Tian Y, Zheng TL, Wang H. Concentration distribution and source of polycyclic aromatic hydrocarbons in surface sediments of Xiamen Western Harbour. *Oceanologia et Limnologia Sinica* 2004; 35 (1): 15-20.
7. Hamer T, Mackay D. Measurement of octanol air partition coefficients for chlorobenzenes, PCBs and DDT. *Environmental Science & Technology* 1995; 29 (6): 1599-1606. doi: 10.1021/es00006a025
8. Liu H, Shi J, Liu H, Wang Z. Improved 3D-QSPR analysis of the predictive octanol-air partition coefficients of hydroxylated and methoxylated polybrominated diphenyl ethers. *Atmospheric Environment* 2013; 77 (3): 840-845. doi: 10.1016/j.atmosenv.2013.05.068
9. Tong JB, Bai M, Zhao X. 3D-QSAR and docking studies of HIV-1 protease inhibitors using R-group search and Surflex-dock. *Medicinal Chemistry Research* 2016; 25 (11):2619-2630. doi: 10.1007/s00044-016-1701-0
10. Zhang AQ, Chen EQ, Wei DB, Wang LS. QSAR research of chlorinated aromatic compounds toxicity to *Selenastrum capricornutum*. *China Environmental Science* 2000; 20 (2): 102-105.
11. Wang C, Lu GH, Tang ZY, Guo XL. Quantitative structure-activity relationships for joint toxicity of substituted phenols and anilines to *Scenedesmus obliquus*. *Journal of Environmental Sciences* 2008; 20 (1): 115-119. doi: 10.1016/s1001-0742(08)60018-2
12. Jackson SH, Cowan-Ellsberry CE, Thomas G. Use of quantitative structural analysis to predict fish bioconcentration factors for pesticides. *Journal of Agricultural and Food Chemistry* 2009; 57 (3): 958-967. doi: 10.1021/jf803064z
13. Liu GS, Song XF, Yu JG, Qian XH. Soil sorption coefficient prediction of substituted phenylureas by artificial neural networks. *Acta Scientiae Circumstantiae* 2002; 22 (3): 359-363. doi: 10.1007/s11769-002-0041-9
14. Lu P, Wei X, Zhang RS. CoMFA and CoMSIA 3D-QSAR studies on quionolone caroxylic acid derivatives inhibitors of HIV-1 integrase. *European Journal of Medicinal Chemistry* 2010; 45 (8): 3413-3419. doi: 10.1016/j.ejmech.2010.04.030
15. Zhao CY. Applications of QSAR in life analytical chemistry and environmental chemistry. PhD, Lanzhou University, Lanzhou, China, 2006 (in Chinese with an abstract in English).
16. Raha K, Peters MB, Yu N, Wollacott AM, Westerhoff LM et al. The role of quantum mechanics in structure-based drug design. *Drug Discovery Today* 2007; 12 (17): 725-731. doi: 10.1016/j.drudis.2007.07.006
17. Kubinyi H. Structure-based design of enzyme inhibitors and receptor ligands. *Current Opinion in Drug Discovery & Development* 1998; 1 (1): 14-15.
18. Tsezos M, Bell JP. Comparison of the biosorption and desorption of hazardous organic pollutants by live and dead biomass. *Water Research* 1989; 23 (5): 561-568. doi: 10.1016/0043-1354(89)90022-5

19. Liu HX, Hu RJ, Zhang RS, Yao XJ, Liu MC et al. The prediction of human oral absorption for diffusion rate limited drugs based on heuristic method and support vector machine. *Journal of Computer-Aided Molecular Design* 2005; 19 (1): 33. doi: 10.1007/s10822-005-0095-8
20. Zhou JJ, Chen HM, Xie GR, Ren TR, Xu ZH. The receptor site model method in 3D-QSAR research. *Progress In Chemistry* 1998; 10 (1): 55-61. doi: 10.3321/j.issn:1005-281X.1998.01.005
21. Kubinyi H. QSAR and 3D QSAR in drug design Part 2: applications and problems. *Drug Discovery Today* 1997; 2 (12): 538-546. doi: 10.1016/S1359-6446(97)01084-2
22. Briens F, Bureau R, Rault S. Applicability of CoMFA in ecotoxicology: a critical study on chlorophenols. *Ecotoxicology and Environmental Safety* 1995; 31 (1): 37-48. doi: 10.1006/eesa.1995.1041
23. Recanatini M, Cavalli A, Belluti F, Piazzini L, Rampa A, et al. SAR of 9-amino-1,2,3,4-tetra-hydroacridine-based acetyl cholinesterase inhibitors: synthesis, enzyme inhibitory activity, QSAR, and structure-based CoMFA of terrine analogues. *Journal of Medicinal Chemistry* 2000; 43 (10): 2007-2018. doi: 10.1021/jm990971t
24. Baurin N, Vangrevelinghe E, Morin-Allory L, Méroux JY, Renard P et al. 3D-QSAR CoMFA study on imidazolinergic  $I_2$  ligands: a significant model through a combined exploration of structural diversity and methodology. *Journal of Medicinal Chemistry* 2000; 43 (6): 1109-1122. doi: 10.1021/jm991124t
25. Kuzmin VE, Artemenko AG, Lozitsky VP, Muratov EN, Fedtchouk AS et al. The analysis of structure-anticancer and antiviral activity relationships for macrocyclic pyridinophanes and their analogues on the basis of 4D QSAR models (simplex representation of molecular structure). *Acta Biochimica Polonica* 2002; 49 (1): 157-168. doi: 10.1016/S0014-5793(01)03245-8
26. Salahinejad M, Ghasemi JB. 3D-QSAR studies on the toxicity of substituted benzenes to *Tetrahymena pyriformis*: CoMFA, CoMSIA and VolSurf approaches. *Ecotoxicology and Environmental Safety* 2014; 105 (1): 128-134. doi: 10.1016/j.ecoenv.2013.11.019
27. Jaworska JS, Comber M, Auer C, Van Leeuwen CJ. Summary of a workshop on regulatory acceptance of (Q)SARs for human health and environmental endpoints. *Environmental Health Perspectives* 2003; 111 (10): 1358-1360. doi: 10.1289/ehp.5757
28. Zhao YY, Gu WW, Li Y. Molecular design of 1,3,5,7-TetraCN derivatives with reduced bioconcentration using 3D-QSAR modeling, full factorial design, and molecular docking. *Journal of Molecular Graphics and Modelling* 2018; 84: 197-214. doi: 10.1016/j.jmgm.2018.07.006
29. Luis P, Ortiz I, Aldaco R, Irabien A. A novel group contribution method in the development of a QSAR for predicting the toxicity (*Vibrio fischeri* EC<sub>50</sub>) of ionic liquids. *Ecotoxicology and Environmental Safety* 2007; 67 (3): 423-429. doi: 10.1016/j.ecoenv.2006.06.010
30. Li Y, Wang D, Yang Y, Zhang J, Han C et al. The 3D-QSAR and pharmacophore studies of pyrimidine derivatives as HCV replication (replicase) inhibitor. *Medicinal Chemistry Research* 2015; 24 (5): 2033-2042. doi: 10.1007/s00044-014-1256-x
31. Gu WW, Chen Y, Li Y. Attenuation of the atmospheric migration ability of polychlorinated naphthalenes (PCN-2) based on three-dimensional QSAR models with full factor experimental design. *Bulletin of Environmental Contamination & Toxicology* 2017; 99 (2): 276-280. doi: 10.1007/s00128-017-2123-5
32. Du MJ, Gu WW, Li XX, Fan FQ, Li Y. Modification of hexachlorobenzene to molecules with lower long-range transport potentials using 3D-QSAR models with a full factor experimental design. *Advances in Marine Biology* 2018; 81 (5): 129-165. doi: 10.1016/bs.amb.2018.09.004
33. Yang XK, Yin XQ, Li HW. The relativity of the quantificational structure of chlorine benzene chemical mopounds in biodegradation. *Journal of Heilongjiang Hydraulic Engineering College* 2006; 33 (1): 97-99. doi: 10.3969/j.issn.2095-008X.2006.01.031 (in Chinese with an abstract in English).

34. Nayana RS, Bommisetty SK, Singh K, Bairy SK, Nunna S et al. Structural analysis of carboline derivatives as inhibitors of MAPKAP K2 using 3D QSAR and docking studies. *Journal of Chemical Information and Modeling* 2009; 49 (1): 53-67. doi: 10.1021/ci800294y
35. Li XM, Zhang QH, Gan YP, Zhou J, Dai JY et al. Bioaccumulation and biomagnification of persistent organic pollutants (POPs) in food chain. *Chinese Journal of Applied & Environmental Biology* 2007; 13 (6): 901-905. doi: 10.3321/j.issn:1006-687x.2007.06.001 (in Chinese with an abstract in English).
36. York PH, Kelaher BP, Booth DJ, Bishop MJ. Trophic responses to nutrient enrichment in a temperate seagrass food chain. *Marine Ecology Progress Series* 2012; 449 (1): 291-296. doi: 10.3354/meps09541
37. Chu ZH, Li Y. Designing modified polybrominated diphenyl ether BDE-47, BDE-99, BDE-100, BDE-183, and BDE-209 molecules with decreased estrogenic activities using 3D-QSAR, pharmacophore models coupled with resolution V of the  $2^{10-3}$  fractional factorial design and molecular docking. *Journal of Hazardous Materials* 2019; 364 (5): 151-162. doi: 10.1016/j.jhazmat.2018.10.027